

## Influence of dust storms on the aerosol optical properties over the Indo-Gangetic basin

Sagnik Dey, Sachchida Nand Tripathi, and Ramesh P. Singh<sup>1</sup>

Department of Civil Engineering, Indian Institute of Technology, Kanpur, India

B. N. Holben

NASA Goddard Space Flight Center, Greenbelt, Maryland, USA

Received 18 April 2004; revised 30 June 2004; accepted 5 August 2004; published 29 October 2004.

[1] Dust storms are considered natural hazards, which affect day-to-day life for a short time from a few hours to a few days. They are common in India especially in the western Rajasthan Province, which is covered by the Thar Desert. In this paper, we present the effects of the dust events on the aerosol parameters retrieved over Kanpur (located in heart of the Indo-Gangetic basin) from ground-based Aerosol Robotic Network (AERONET) measurements. The aerosol parameters show strong seasonal variability in this region, with least spectral dependence of aerosol optical depth (AOD) during the premonsoon season, characterized by dust loading. The aerosol optical properties over the Indo-Gangetic basin are controlled by the diurnal and seasonal cycles of urban pollutants, but the dust storms are so significant that the local cycle is completely overshadowed. A rise in AOD by more than 50% and corresponding decrease in angstrom parameter by 70–90% have been observed after each dust event. The diurnal variations of AOD during the dust events have been found to be controlled by the onset of the dust storms. The changes in the single scattering albedo (SSA) and real  $n(\lambda)$  and imaginary  $k(\lambda)$  parts of the refractive index indicate that the 27 May 2002 event influences the optical state to be absorbing, whereas for the other four events the aerosols are found to be dominantly scattering in nature. SSA has been found to increase sharply at higher wavelengths ( $\lambda > 440$  nm) during the dust events, whereas  $n(\lambda)$  and  $k(\lambda)$  increase 2–3 times more at  $\lambda = 440$  nm compared to those at higher wavelengths. The contrasting change in the spectral variations of the optical properties is due to the difference in the nature of the aerosols loading during the events. Aerosol volume concentration at coarse mode is found to increase three times after the dust events, whereas no significant change has been observed in the volume concentration at fine mode. Concentration of the particulate matters less than  $10 \mu\text{m}$  ( $\text{PM}_{10}$ ) is also found to increase by  $\sim 150 \mu\text{g m}^{-3}$  after each dust event except on the 27 May 2002 event, when heavy rainfall after the dust storm washed out the suspended particulate matters from the atmosphere, and the ground level  $\text{PM}_{10}$  concentration was not influenced by the advected dust particles on that day. Aerosol index values in successive Total Ozone Mapping Spectrometer (TOMS) images over the region support the characterization of the aerosols in this region in terms of their optical properties, which are being transported over the Indo-Gangetic basin from the western Thar Desert and the Gulf regions depending upon the size of the particles, shown by the air mass trajectories. **INDEX TERMS:** 0305 Atmospheric Composition and Structure: Aerosols and particles (0345, 4801); 0345 Atmospheric Composition and Structure: Pollution—urban and regional (0305); 1640 Global Change: Remote sensing; 3309 Meteorology and Atmospheric Dynamics: Climatology (1620); 3360 Meteorology and Atmospheric Dynamics: Remote sensing; **KEYWORDS:** aerosol, dust, India

**Citation:** Dey, S., S. N. Tripathi, R. P. Singh, and B. N. Holben (2004), Influence of dust storms on the aerosol optical properties over the Indo-Gangetic basin, *J. Geophys. Res.*, *109*, D20211, doi:10.1029/2004JD004924.

<sup>1</sup>Temporarily at School of Computational Sciences, George Mason University, Fairfax, Virginia, USA.

### 1. Introduction

[2] Mineral dusts are considered a major contributor to the aerosol loading in the troposphere influencing the seasonal variability of the aerosol optical properties and the local radiative forcing [*Teegen and Lacis*, 1996]. Dusts in

the atmosphere have terrestrial sources and represent an important process of land-atmosphere interaction [Tegen et al., 1996]. Dust storms have considerable impacts on climate variability, nutrient dynamics and biogeochemical cycles of oceans, soil characteristics, and ambient air quality. Numerous studies using satellite and surface observations [Husar et al., 1997, 2001; Prospero, 1999; Prospero et al., 2002; Washington et al., 2003] have shown that the global sources of the atmospheric dusts are the arid and semiarid desert regions contributing to the long-range transport of dust particles lifted by strong surface winds ( $>5 \text{ m s}^{-1}$ ).

[3] The Thar Desert centered in western India and eastern Pakistan is the primary potential source of dusts in the Indian subcontinent [Pease et al., 1998; Léon and Legrand, 2003; Washington et al., 2003]. During the premonsoon period, dust storms are often experienced in different parts of the Indo-Gangetic basin [Middleton, 1986a]. Frequency of the dust storms in northern and northwestern India is maximum during the premonsoon season, when dusts are transported by southwesterly summer winds from the western Thar Desert [Sikka, 1997]. During the winter, dusts are transported to the Arabian Sea (some examples of dust transport over the area during the premonsoon season can be observed through satellite images at <http://visibleearth.nasa.gov/Sensors/Terra/MODIS.html>). High dust loading in the Gangetic basin during the premonsoon season has been established by remote sensing data [Prospero et al., 2002; Washington et al., 2003]. These dust storms apparently deposited silty materials in the downwind directions, as observed on the quartzite ridges in the Delhi area [Tripathi and Rajamani, 1999]. The wind also carries heavy metals to the Indo-Gangetic basin during the summer season [Yadav and Rajamani, 2003] along with the dusts, causing severe air pollution and degradation in the visibility.

[4] The aerosol optical properties affect the local radiative forcing, which is the most uncertain component of the Earth-atmosphere system [Hansen et al., 1997; Sathesh et al., 1999]. The mineral aerosols having very large surface area strongly absorb the shortwave solar radiation [Dickerson et al., 1997] and cause photolysis rate reduction inhibiting the ozone production [Bonasoni et al., 2004]. They also influence the balance of atmospheric trace gases and ozone [Prospero et al., 1995; Dickerson et al., 1997].

[5] The Indo-Gangetic basin is dominated by the urban/industrial aerosols [Guttikunda et al., 2003; Sharma et al., 2003; Monkkonen et al., 2004], which demonstrate significant seasonal variability based on the complex combination of anthropogenic factors mixed with the contribution from the natural sources, particularly in the premonsoon and monsoon seasons. Before the onset of the monsoon, relative humidity varies in a wide range (dry in northern India and humid in the eastern part) with a considerable heat wave running across the region. The growing urbanization and economic growth in the Indo-Gangetic basin result in significant increase in the air pollution [Guttikunda et al., 2003] in the region. Measurements by the Central Pollution Control Board (CPCB) of India have shown that the concentration of particulate matter of diameter  $<10 \mu\text{m}$  ( $\text{PM}_{10}$ ) is above the critical level ( $>150 \mu\text{g m}^{-3}$ ) in many big industrial cities of the Indo-Gangetic basin like Kanpur,

Delhi, and Kolkata [Mitra and Sharma, 2002]. A study by Sharma et al. [2003] has shown that the high  $\text{PM}_{10}$  concentration provides an opportunity for  $\text{SO}_4$  formation on the particulate surface, leading to very high concentration of sulfate aerosols in the atmosphere, which is the case in the Indo-Gangetic basin. It is interesting to study how the naturally transported dusts modify the optical properties in this region. Moreover, dust particles are nonspherical, which affect the accuracy of the retrieval of the aerosol optical properties [Mishchenko et al., 1995] during the premonsoon season. The dusts transported to the Indo-Gangetic basin every year during summer season affect the ambient air quality of the region. Though the dust storms in the Indian subcontinent received some attention [Joseph, 1982; Middleton, 1986b; Negi et al., 1996] in the past, their effect on the aerosol optical properties in the region has not been studied with a continuous data set.

[6] In the present study, we present the analyses of optical properties of the aerosols during 1 May to 16 May 2001 and 18 May to 31 May 2002. During this period, five intense dust events are observed on 8 and 9 May in 2001 and 19, 20, and 27 May in 2002. Analyses for the dust storms in May 2003 have not been included as level 2.0 data of the aerosol optical and microphysical properties are not available during this time period. The dust storms show significant impact on the aerosol optical properties in the region.

## 2. Instrumentation and Data

[7] Aerosol optical properties over Kanpur are being monitored continuously as of January 2001 by CIMEL sky radiometer, deployed on the campus of the Indian Institute of Technology (IIT), Kanpur, India ( $80^{\circ}20'E$ ,  $26^{\circ}26'N$  and 142 m altitude from mean sea level), as a part of the Aerosol Robotic Network (AERONET) program under the collaboration with NASA and IIT Kanpur. Kanpur is chosen as a representative site of the Indo-Gangetic basin, as it is situated in the central part of the basin. The CIMEL radiometer is located on top of a roof with no obstructions to the Sun above  $10^{\circ}$  elevation; it takes measurements of the direct Sun and diffuse sky radiance with  $1.2^{\circ}$  full field of view within the spectral range 340–1020 nm [Holben et al., 1998]. The direct Sun measurements are made at eight spectral channels (340, 380, 440, 500, 670, 870, 940, and 1020 nm) with triplet observations per wavelength and sky radiance measurements at four spectral channels (440, 670, 870, and 1020 nm). Water vapor content in the atmosphere is retrieved from the direct measurements at the 940-nm channel, and aerosol optical depth (AOD) data are retrieved at the remaining seven channels. Two basic sky radiance observation modes, almucantar and principle plane, are used to retrieve the size distribution, single scattering albedo (SSA), and refractive indices of the aerosols [Holben et al., 1998].

[8] The uncertainty in calculation of AOD under cloud-free conditions is  $< \pm 0.01$  for  $\lambda > 440 \text{ nm}$  and  $< \pm 0.02$  for shorter wavelengths,  $\pm 10\%$  for retrieval of cloud water vapor, and is  $< \pm 5\%$  for the sky radiance measurements. The Sun and sky radiance measurements yield two types of errors, systematic and random [Dubovik et al., 2000]. These errors depend on the nature of the aerosols. Even in the so-called error-free conditions (neither systematic nor random

errors are specifically introduced in the forward simulations or in the inversion algorithms), some minor errors exist, which can be considered relative errors with standard deviation <1% for all three water-soluble, dust and biomass-burning aerosol models [Dubovik *et al.*, 2000]. It is notable that errors are significant only for both fine (particle radius  $R < 0.1 \mu\text{m}$ ) and coarse ( $R > 7 \mu\text{m}$ ) sizes. The tendency of increasing errors in retrieval of optical properties with the decrease in optical depth is higher in the case of refractive index and SSA than for the case of volume size distribution [Dubovik *et al.*, 2000]. The detailed analyses of the retrieval accuracy for different kinds of aerosols from the Sun and sky radiance measurements by the CIMEL sky radiometer have been discussed by Dubovik *et al.* [2000]. The AOD data are provided in three categories, cloud contaminated (level 1.0), cloud screened (level 1.5), following the methodology described by Smirnov *et al.* [2000], and quality assured (level 2.0). Level 2.0 data have been used for this study. The aerosol optical properties have been retrieved using nonspherical particle models of Mishchenko *et al.* [1997] for better understanding on the effects of the dust events on the regional aerosol optical properties.

[9]  $\text{PM}_{10}$  concentration data are available from CPCB (<http://cpcb.nic.in>). Daily  $\text{PM}_{10}$  concentration is measured over 295 locations in India under the National Ambient Air Quality Monitoring program (NAAQM) through a high-volume sampler. Under the NAAQM program, four air pollutants ( $\text{PM}_{10}$ , suspended particulate matter,  $\text{SO}_2$ , and  $\text{NO}_x$ ) are routinely monitored at all stations. The  $\text{PM}_{10}$  data considered close to the IITK AERONET site are within <10 km, which is routinely monitored by the CPCB. The location is within an urban area, influenced by local transportation.

[10] The  $\text{PM}_{10}$  data are collected following the protocols developed under NAAQM. Air is drawn through a size-selective inlet and a  $20.3 \times 25.4 \text{ cm}$  filter at a flow rate of about  $1000 \text{ L min}^{-1}$ . Particles with aerodynamic diameter less than the cut-off point of the inlet are collected by the filter. The mass of these particles is determined by the difference in filter weights prior to and after sampling. The concentration of  $\text{PM}_{10}$ , in the designated size range, is calculated by dividing the weight gain of the filter by the volume of air sampled. For a 24-hour sample duration at about average  $1000 \text{ L min}^{-1}$ , the lowest detection limit is determined by the reproducibility of the filter weight difference which shows a standard deviation ( $\sigma$ ) of approximately  $\pm 2 \text{ mg}$ . The three- $\sigma$  detection limit is approximately  $3.5 \mu\text{g m}^{-3}$ . The three- $\sigma$  lower quantifiable limit depends on the filter used and may be even  $5 \mu\text{g m}^{-3}$ . For 24-hour sample duration at about  $1000 \text{ L min}^{-1}$  the upper quantifiable limit is  $1000 \mu\text{g m}^{-3}$ . However, the exact value depends on the nature of the aerosol being sampled; very small particles will clog the filter at a relatively low mass loading, while larger particles will bounce off during sample transport at high concentrations. The sampler is periodically calibrated, at least once a year or whenever a major repair/replacement of the blower takes place, by using a top-loading calibrator traceable to national standard.

[11] The aerosol index (AI) data derived from the Total Ozone Mapping Spectrometer (TOMS) have been used to support the characterization of the aerosols in the region. TOMS AI is a qualitative indicator of ultraviolet absorbing

aerosols [Herman *et al.*, 1997; Torres *et al.*, 1998]. Non-absorbing aerosols (e.g., water-soluble and sea-salt particles) yield negative or very low positive AI values, whereas ultraviolet absorbing aerosols (e.g., dust, smoke, and biomass burning) yield positive values. Global studies have shown that typical AI values for major dust sources retrieved from TOMS lie in the range 0.5–3.0 [Prospero *et al.*, 2002; Washington *et al.*, 2003].

### 3. Seasonal Variation of Aerosol Parameters

[12] The Indo-Gangetic basin is one of the most polluted regions in the world [Guttikunda *et al.*, 2003]. In the Indo-Gangetic basin, four seasons dominate annually, winter (December–February), premonsoon (March–May), monsoon (June–August), and postmonsoon (September–November). Seasonal variations of AOD at 500-nm wavelength ( $\tau_{a,500}$ ) and the angstrom parameter ( $\alpha$ ) over Kanpur are shown in Figure 1a. Aerosol parameters are characterized by AOD, whose spectral dependence is quantified by  $\alpha$  deduced from a multispectral log linear fit to the classical equation of Angstrom [Angstrom, 1964] in the wavelength range 440–870 nm. Here  $\alpha$  can be considered as a first-order indicator of the average spectral behavior. Higher value of  $\alpha$  indicates dominance of fine-mode particles with higher spectral variation in AOD;  $\tau_{a,500}$  in the region is higher than 0.35 throughout the year. Maximum  $\tau_{a,500}$  has been observed during the premonsoon seasons ( $>0.8$ ) corresponding to the maximum decrease in  $\alpha$ . The notable decrease in  $\alpha$  is attributed to the abundance of coarse particles arising because of dust loading. During the other seasons,  $\tau_{a,500}$  is variable with  $\alpha > 0.8$ . Only in 2002, has the reduction in spectral variation of AOD been observed during the monsoon season. The spectral variations in AOD during 3 years show a systematic pattern in aerosol loading in the region, strongly influenced by seasonal variability. A synoptic air mass flowing southwesterly during premonsoon season results in frequent dust loading, whereas urban aerosols are being loaded in the atmosphere throughout the year. During the winter season,  $\tau_{a,500}$  has been found to be minimum.

[13] The interaction of the aerosol particles strongly depends on the size factor, i.e., the ratio of the aerosol size to the incident wavelength and the refractive index. Therefore, in order to understand the effects of the aerosols on the solar radiation, it is important to characterize the size distribution. Volume size distribution averaged over 2 years (2001–2002) is illustrated in Figure 1b, which shows strong seasonal influence. The size distribution is bimodal, and the volume concentration increases with the increase in AOD. The fine mode varies in the range 0.08–0.2  $\mu\text{m}$ , and the coarse mode is centered around 5  $\mu\text{m}$ . The fine mode is found to shift toward the coarser side during the postmonsoon and winter seasons (from particle radius  $R = 0.1$ –0.4  $\mu\text{m}$ ), whereas no shift has been observed for the coarse mode. The bimodal structure of volume size distribution may be due to various reasons, like mixing of two air masses with different aerosol populations [Hoppel *et al.*, 1985], homogeneous heteromolecular nucleation of new fine particles in the air, or heterogeneous nucleation and growth of larger particles by condensation of gas phase

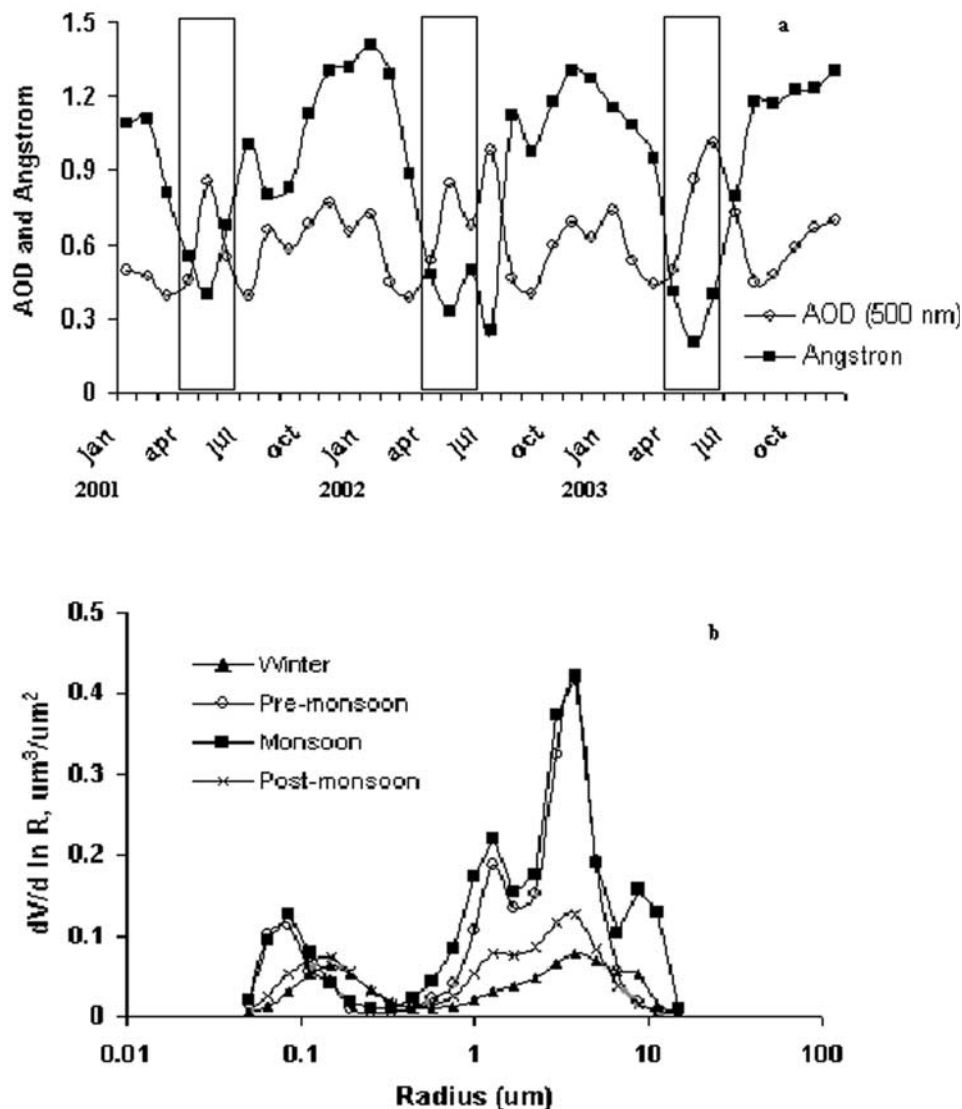


**Figure 1.** (a) Seasonal variations in aerosol optical depth (AOD) at 500-nm wavelength  $\tau_{a,500}$  and angstrom parameter over Kanpur during 2001–2003. The boxes represent the premonsoon season. (b) Seasonal aerosol volume size distribution over Kanpur.

reaction products. The changes in spectral dependency of AOD due to the loading of different kinds of particles are reflected in the aerosol size distribution [O'Neill *et al.*, 2001]. Volume concentrations in the fine and coarse mode are almost equal during the postmonsoon and winter seasons, whereas the volume concentration in the coarse mode is much higher than that at the fine mode during the premonsoon and monsoon seasons. This indicates the dominance of the coarser particles during the premonsoon and monsoon seasons in the atmosphere over the region, whereas both fine and coarse particles are present in other seasons. The sources of the fine aerosol particles are the pollutants being emitted from industries and automobiles. It is interesting to find a third mode (lower volume concentration than the two main modes) in the size distribution during the premonsoon and monsoon seasons, which arises because of the hygroscopic growth of fine nucleation mode particles in the presence of high relative humidity [Parameswaran and Vijayakumar,

1994; Kotchenruther *et al.*, 1999]. Basically, during the premonsoon to monsoon seasons the size distribution reveals all three modes, nucleation ( $<0.1 \mu\text{m}$ ), accumulation ( $0.1–2 \mu\text{m}$ ), and coarse mode ( $>2 \mu\text{m}$ ). Coarse particles are generated by mechanical processes and consist of wind-blown dust, plant pollens, and other sources. During the premonsoon and monsoon seasons, dust transported over the Indo-Gangetic basin increases volume concentration in the coarse mode in the range  $0.4–0.5 \mu\text{m}^3 \mu\text{m}^{-2}$  from the values of  $0.1–0.2 \mu\text{m}^3 \mu\text{m}^{-2}$  observed in the winter and postmonsoon seasons. However, the volume concentration at the fine mode remains in the range of  $0.5–0.15 \mu\text{m}^3 \mu\text{m}^{-2}$  in all four seasons.

#### 4. Results and Discussions

[14] Aerosol optical and microphysical properties have been studied during the period of the dust events observed during May 2001 and 2002. The effect of the dust events on

the aerosol optical properties in the Indo-Gangetic basin is discussed in section 4.1.

#### 4.1. Aerosol Optical Depth Spectra and Angstrom Parameter

[15] The temporal variations of  $\tau_{a,500}$  and  $\alpha$  during May 2001 and May 2002 are shown in Figures 2a and 2b, respectively. The monthly averages of  $\tau_{a,500}$  and  $\alpha$  are found to be 0.821 and 0.838 and 0.4 and 0.33 during May 2001 and 2002, respectively. After the dust events on 8 and 9 May 2001,  $\tau_{a,500}$  has been observed to be 1.28, whereas after the events on 19–20 and 27 May 2002, it has been found to be 1.7 and 1.48, respectively. In the case of all five events, AOD rises above 1 even at the lowest wavelength ( $\lambda = 340$  nm, not shown in Figure 2). A sharp increase in AOD by 0.4–0.7 at all the wavelengths has been observed on the days of dust events with significant reduction in the spectral dependency showing very little sensitivity to wavelengths. As a result,  $\alpha$  tends to decrease below 0.25 immediately after the events. The dust events in all 5 days contribute to the increase in AOD by 50–100% and decrease in  $\alpha$  by 70–90%. This sharp decrease in  $\alpha$  is due to the extinction of incoming solar radiation at the visible and infrared wavelengths by dust particles, resulting in small and even negative values [Hamonou *et al.*, 1999]. Smirnov *et al.* [1998] have shown similar behavior, decrease in  $\alpha$  from 1.5 to 0.14 and increase of AOD at 500 nm from 0.1 to 0.4 (300% rise) during the Saharan dust events. Common spectral variation of AOD shows higher values at lower wavelengths, indicating more abundance of finer particles [Eck *et al.*, 1999]. The domination of large particles ( $r > 0.6$   $\mu\text{m}$ ) in the dust aerosol enhances the interaction of the incoming solar radiation at the higher wavelengths ( $\lambda > 600$  nm), as a result, AOD at  $\lambda > 600$  nm increases largely compared to AOD at lower wavelengths, showing a decrease in the wavelength dependency. Similar results have been observed by Tanre *et al.* [2003], where maximum AOD associated with minimum  $\alpha$  has been found over a station closest to the dust sources. During the period of the study, AOD has been observed to increase above 0.9, and  $\alpha$  is found to decrease to 0.24 on 14 May 2001, indicating another mild dust storm not affecting much of the spectral dependency compared to the other five events.

#### 4.2. Single Scattering Albedo

[16] Particulate scattering is the most important process of solar radiation attenuation in the polluted environment, which is represented by SSA. The details of retrieval of SSA from Sun and sky radiance measurements by CIMEL Sun photometer are discussed by Dubovik and King [2000]. Figures 2c and 2d show the daily variations of SSA at four wavelengths (440, 670, 870 and 1020 nm) prior to and after the dust storms over Kanpur. The average values of SSA at 670-nm wavelength are found to be 0.906 and 0.948 during May 2001 and 2002, respectively, indicating that the season is dominated by the presence of scattering aerosols. Sharma *et al.* [2003] have shown that the abundance of particulate matters in the atmosphere facilitates the formation of sulfate aerosols from the very high concentration of  $\text{SO}_2$  emitted in this region. The dominance of the water-soluble aerosols in this region attributes to the high monthly average SSA, quite similar to the values in the range 0.82–0.97 obtained

during the Tropospheric Aerosol Radiative Forcing Observational Experiment (TARFOX) [Hegg *et al.*, 1997; Russell *et al.*, 1999; Hartley *et al.*, 2000]. These values are found to be higher than the values retrieved by several models [Shettle and Fenn, 1979; World Meteorological Organization (WMO), 1983; Koepke *et al.*, 1997; Hess *et al.*, 1998], suggesting less absorption by the dust particles transported over the Indo-Gangetic basin. Presence of iron oxide and silica in the dust particles is responsible for absorption [Dubovik *et al.*, 2002a], though dust particles mostly scatter the light impinging on them.

[17] The dust events of May 2001 and 19 and 20 May 2002 show a small increase of SSA, 0.01–0.04, whereas after the 27 May 2002 event, SSA has been found to decrease by 0.07. Maximum increase in SSA has been associated with the strongest event on 20 May 2002. The changing nature of SSA during these events shows that the first four events have a strong impact on the optical properties compared to the 27 May 2002 event. The small increase in SSA is due to the abundant dust loading in the region, attributing to the scattering state of the atmosphere; with the presence of absorbing nature of dusts, SSA shows very small change (Figure 2d). In comparison, a decrease in SSA values at all wavelengths after the 27 May 2002 event proves the dominant absorbing state of the atmosphere, arising because of the absorbing aerosols (soot and biomass burning), which are abundant in the eastern part of India [Reddy and Venkataraman, 2002]; as a result the effect of the dust storm has been overshadowed. The western Thar Desert is the main source of the dusts in this region; the idea of the changing nature of the dust composition in such a short span of time does not work. SSA values of the absorbing aerosols (mainly biomass burning) are higher at the lower wavelength [Dubovik *et al.*, 2002a]. After the 27 May 2002 dust event the spectral variation of SSA has been observed to reduce significantly, clearly showing the effects of the absorbing aerosol loading.

[18] SSA during the study period shows strong spectral variation, with higher values at the higher wavelengths. SSA spectra show a steep rise in the values from 440-nm to 670-nm wavelengths during the dust event days, which clearly suggests more scattering at  $\lambda > 670$  nm due to the increase in the number of coarse particles (Figures 2a and 2b). This SSA spectrum is associated with the higher increase in AOD at larger wavelengths during the dust storms. The steepness of SSA spectra has been found to be reduced in the nondust event days in accordance with the size distribution and the AOD spectrum.

#### 4.3. Index of Refraction

[19] The refractive index is an important optical parameter, highly dependent on the chemical composition of the aerosols. The refractive index is a complex quantity, expressed in terms of real  $n(\lambda)$  and imaginary  $k(\lambda)$  parts;  $n(\lambda)$  and  $k(\lambda)$  give an indication about the absorption properties of aerosols. A typical value of  $n(\lambda)$  of the dust based on several models is taken as 1.53 in the visible spectrum [Shettle and Fenn, 1979; WMO, 1983; Koepke *et al.*, 1997] for calculation of radiative transfer of energy. However, the value may deviate within a range of  $\pm 0.05$  because of the difference in the dust composition and the difference in measurement technique [Sokolik *et al.*, 1993;

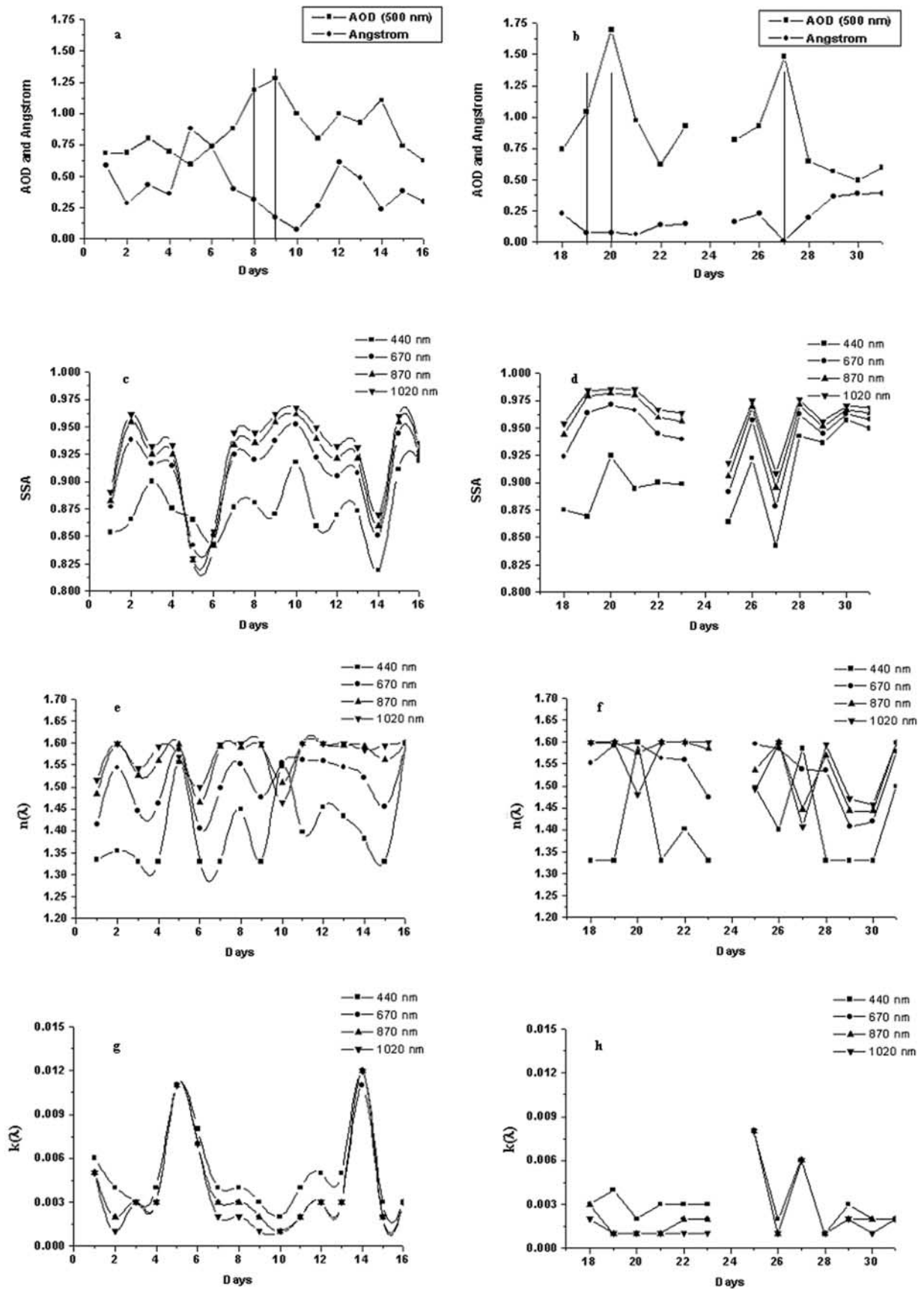
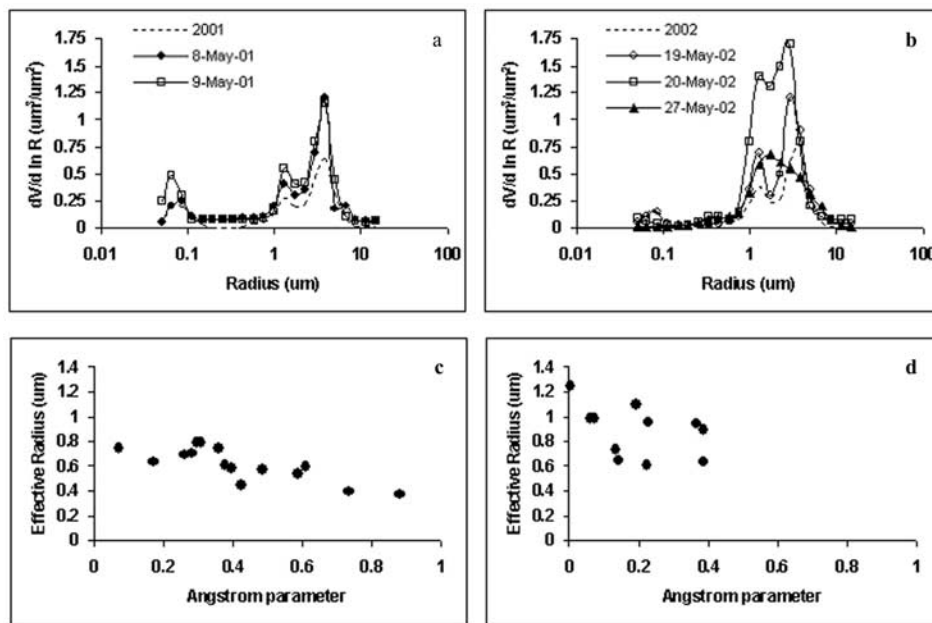


Figure 2



**Figure 3.** Aerosol volume size distribution on the days of the dust storms in May (a) 2001 and (b) 2002. Effective radius,  $R_{\text{eff}}$  of the total size distribution as a function of the angstrom parameter during May (c) 2001 and (d) 2002.

*Sokolik and Toon*, 1999]. Similarly, the value for  $k(\lambda)$  for dust in the visible spectrum is calculated to be 0.006 by several models [*Shettle and Fenn*, 1979; *WMO*, 1983], though lower values are also reported [*Levin et al.*, 1980; *Otterman et al.*, 1982].

[20] Spectral variations of  $n(\lambda)$  and  $k(\lambda)$  are shown in Figures 2e–2h. These values are similar to the values reported by several workers [*Shettle and Fenn*, 1979; *Levin et al.*, 1980; *Otterman et al.*, 1982; *WMO*, 1983; *Koepke et al.*, 1997]. The average  $n(\lambda)$  and  $k(\lambda)$  at 670-nm wavelength for the month of May are found to be 1.495 and 0.004 and 1.541 and 0.002 in 2001 and 2002, respectively. Changes in  $n(\lambda)$  and  $k(\lambda)$  are observed to be more at the lower wavelength. The  $k(\lambda)$  values at 440-nm wavelength is 2–3 times higher than at higher wavelength, which is not surprising for the dusts [*Sokolik et al.*, 1993; *Koepke et al.*, 1997; *Sokolik and Toon*, 1999]. In fact, the  $k(\lambda)$  values at 870-nm and 1020-nm wavelengths are almost similar in both years. Spectral variation of  $n(\lambda)$  is found to increase, whereas  $k(\lambda)$  is found to decrease after all the dust events except the 27 May 2002 event. The increase of  $n(\lambda)$  indicates an increase of total scattering [*Bohren and Huffman*, 1983]. Sharp changes in the values of both  $n(\lambda)$  and  $k(\lambda)$  after the dust events of May 2001 and the first two events of May 2002 indicate an increase in the scattering state of the atmosphere, which is also reflected in the changing nature of SSA. In contrast, the 27 May 2002 event shows an increase in the absorbing state of the atmosphere, which is reflected by the decrease of  $n(\lambda)$

and increase of  $k(\lambda)$ . However, it is noteworthy that the change in  $n(\lambda)$  at 440-nm wavelength is opposite to the change at the other wavelength, which means the optical properties at the shorter wavelength have not been affected by the dust storms. After 27 May 2002 the decrease in  $n(\lambda)$  is coherent at all the wavelengths, because the presence of both fine absorbing and coarse scattering aerosols affect all the wavelengths. The changing behavior of the optical state of the aerosols during the dust events is also supported by the SSA values. The spectral variation of  $k(\lambda)$  becomes minimal on 27 May 2002 compared to the other days with higher values at the lower wavelength. Although the spectral response of  $k(\lambda)$  is not similar to that of  $n(\lambda)$ , the dust storms result in reducing the spectral variation of  $k(\lambda)$  at the higher wavelengths ( $\lambda > 440$  nm) more effectively.

#### 4.4. Aerosol Size Distribution

[21] In practice, most plausible size distributions of spheres and spheroids can be represented by effective radius  $R_{\text{eff}}$  and geometric standard deviation  $\sigma$  [*Hansen and Travis*, 1974; *Mishchenko and Travis*, 1994]. The nonsphericity of the dust particles affects the retrieval methodology of the optical properties of the aerosols [*Mishchenko et al.*, 1995, 2000; *Dubovik et al.*, 2002b]. The size distribution parameters shown in Figures 3 have been deduced using the nonspherical models on the almucantar sky radiance measurements proposed by *Dubovik et al.* [2002b].

[22] The abundance of coarse-mode particles (particle radius,  $R > 0.6 \mu\text{m}$ ) in the dusts is the primary character,

**Figure 2.** Daily variation of AOD at 500-nm wavelength  $\tau_{a,500}$  and angstrom parameter in May (a) 2001 and (b) 2002. Vertical bars represent the days of the dust events. Daily variation of single scattering albedo (SSA) at four wavelengths in May (c) 2001 and (d) 2002. Daily variation of real refractive indices at four wavelengths in May (e) 2001 and (f) 2002. Daily variation of imaginary refractive indices at four wavelengths in May (g) 2001 and (h) 2002.

**Table 1.** Observed Daily and Monthly Average Volume Size Distribution Parameters of Aerosol Particles<sup>a</sup>

Date	$V_c$	$R_{\text{eff},c}$	$\sigma_c$	$V_f$	$R_{\text{eff},f}$	$\sigma_f$
8 May 2001	1.0441	2.306	0.57	0.082	0.094	0.116
9 May 2001	1.086	2.256	0.528	0.088	0.076	0.73
May 2001	0.633	2.237	0.56	0.0944	0.091	0.576
19 May 2002	1.083	2.154	0.562	0.063	0.09	0.8
20 May 2002	2.253	1.841	0.527			
27 May 2002	1.583	1.96	0.624	0.073	0.131	0.837
May 2002	1.083	2.289	0.53	0.063	0.09	0.8

<sup>a</sup> $V_c$  and  $V_f$  are the columnar volume of coarse and fine particles, respectively, per unit cross section of the atmospheric column;  $R_{\text{eff},c}$  and  $R_{\text{eff},f}$  are effective radii at coarse and fine mode, respectively; and  $\sigma_c$  and  $\sigma_f$  are the geometric standard deviation of the coarse and fine modes, respectively.

which differentiates the optical properties of dusts with the urban and biomass-burning aerosols [Dubovik *et al.*, 2002a]. The aerosol volume size distribution ( $dV/d \ln R$ ) has been retrieved from the spectral Sun and sky radiance data following the approach discussed by Dubovik and King [2000] with the initial guess:  $dV/d \ln R = 0.0001$ ,  $n(\lambda) = 1.5$ ,  $k(\lambda) = 0.005$ ; where  $dV/d \ln R$  denotes volume size distribution,  $n(\lambda)$  and  $k(\lambda)$  are the real and imaginary parts of the refractive index at wavelength  $\lambda$ , respectively. Figures 3a and 3b show the daily variations of aerosol volume size distribution during the dust events in May 2001 and 2002, respectively. The observed daily and monthly average volume size distribution is found to be bimodal; the volume size distribution parameters are given in Table 1. Monthly average volume concentration in the coarse ( $V_c$ ) and fine mode ( $V_f$ ) are found to be 0.633 and 0.0944 and 1.083 and 0.063 in May 2001 and 2002, respectively. After the dust events of 8 and 9 May 2001 and 20 May 2002,  $V_c$  has been found to increase almost two times without much change in the effective radius at the coarse-mode  $R_{\text{eff},c}$ . The monthly average values of  $R_{\text{eff},c}$  are found to be 2.237 and 2.289  $\mu\text{m}$  in 2001 and 2002, respectively. Average values of the effective radius at the fine mode,  $R_{\text{eff},f}$  are found to be 0.091 and 0.09  $\mu\text{m}$  during May 2001 and 2002, respectively, which suggests a similar pattern of loading of finer urban aerosols during this season.

[23]  $R_{\text{eff}}$  of the total size distribution for May 2001 and 2002 are shown as function of  $\alpha$  in Figures 3c and 3d, respectively. For large particles,  $R_{\text{eff}}$  is representative of the optical properties [Tanre *et al.*, 2001].  $R_{\text{eff}}$  has been found to decrease with the increase in  $\alpha$ . This clearly indicates that during the dust storms the AOD spectra are totally dominated by the coarse particles, which have a significant impact on the observed aerosol volume size distribution. Though the trends of  $R_{\text{eff}}$  are similar in both May 2001 and 2002, the linear correlation is poor in 2002 ( $R = 0.2$ ) compared to that in 2001 ( $R = 0.65$ ). This is due to that fact that dust events in the year 2002 suffer more severe dust loading compared to the dust events of 2001, which allows  $R_{\text{eff}}$  to remain high ( $>0.4 \mu\text{m}$ ) even on the nondust days. Maximum increase in  $V_c$  has been found on 20 May 2002, which was the most intense dust storm during 2001–2002, also evident from the sharp rise of AOD (Figure 2b). Dust events of 19 and 27 May 2002 do not show a significant change in  $V_c$  compared to the monthly average.  $V_f$  is almost similar to the monthly average on the dust event days, which means no significant increase in the loading of fine particles during the events. The variation of  $R_{\text{eff},f}$  values during the dust events suggests minimum impact of the dust

storms on the particle size distribution at the fine mode.  $R_{\text{eff},f}$  has been found to increase from a monthly average of 0.09  $\mu\text{m}$  to 0.131  $\mu\text{m}$  on 27 May 2002. This is attributed to the transport of the fine absorbing aerosols from the eastern part of the basin, resulting in a shift of the modal peak of the size distribution curve at the coarse mode toward the finer fraction.

#### 4.5. Diurnal Variation of $\tau_{a,500}$

[24] The diurnal variations of  $\tau_{a,500}$  (Figure 4) indicate seasonal influence on aerosol loading. Diurnal variations of  $\tau_{a,500}$  during the dust storms are shown as percentage departure from the daily average (Figure 4). During the premonsoon season, maximum diurnal variations have been observed in the morning and the afternoon. Such diurnal variation has been observed over the sites where dust is the major contributor to optical depth [Smirnov *et al.*, 2002]. However, during the days of dust events, diurnal variation has been found to be completely different. On 8 May 2001 and 19 and 27 May 2002 the events took place early in the day, resulting in maximum departure of AOD from the average before local noon (at 1200 hours), whereas the 9 May 2001 and 20 May 2002 events took place in the afternoon. The diurnal cycle of the pollutants emitting from the local industrial and automobile sources is completely overshadowed during dust storm days because of huge loading of the long-range dust transport.

[25] The local diurnal cycle of aerosol loading and the seasonal variations of the aerosol are found to show significant dependence on the ambient meteorological conditions (namely, temperature, relative humidity, and wind speed) (Figures 5a and 5b). The variation of daily averaged

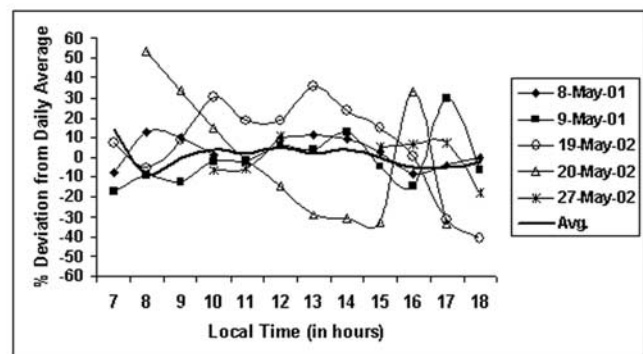


**Figure 4.** Diurnal variations of  $\tau_{a,500}$  during the dust event days along with the seasonal average.

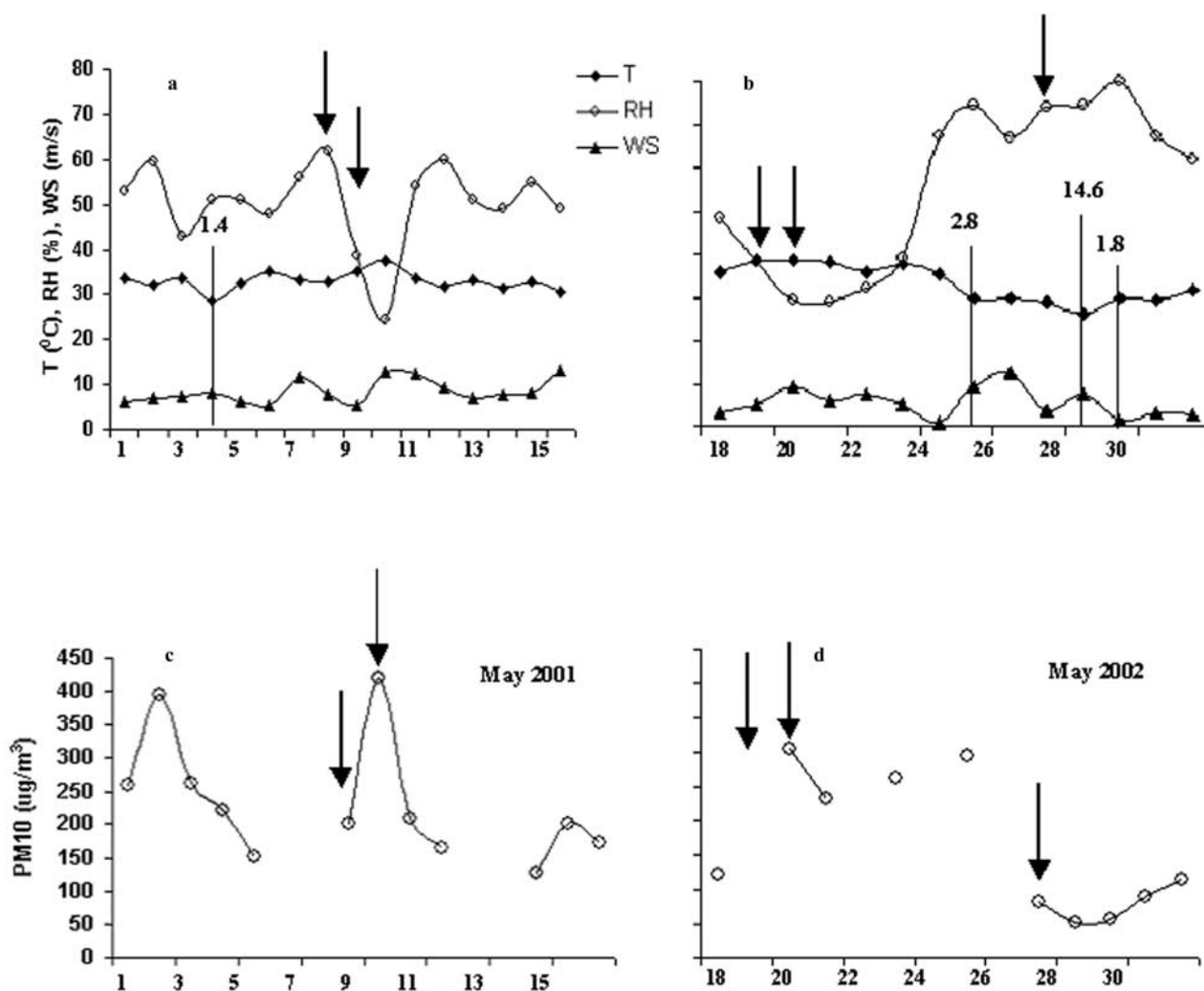


**Figure 5.** Variations of temperature (T) (in °C), relative humidity (RH) (in percent) and wind speed (WS) (in  $\text{m s}^{-1}$ ) in (a) May 2001 and (b) May 2002. The arrows indicate the days of the dust events, and the vertical lines represent the days of the precipitation, with the amount indicated on top of the lines. Daily variation of  $\text{PM}_{10}$  concentration in May (c) 2001 and (d) 2002.

temperature is not very high during the study period, but the diurnal variation is quite high. This leads to the enhancement of the local diurnal cycle. In the nighttime, aerosols are trapped in the nocturnal stable layer, and with the increase in temperature in the daytime the mixed layer starts to grow from the surface. The local pollutants, emitted from the industries and the automobiles during the daytime, are entrained into the mixed layer, causing high diurnal variation of AOD. During the dust events, huge fluxes of the dusts are transported from a long distance, as a result the daily average AOD is found to increase. The dust storms occurring in the afternoon suppress the local diurnal cycle. Decrease in relative humidity is observed after the dust events, except the 27 May 2002 event (Figures 5a and 5b), which is due to the transport of the dry air mass carrying the soil dusts into the region. Wind speed has been found to be greater than  $5 \text{ m s}^{-1}$  during dust event days.

#### 4.6. $\text{PM}_{10}$ Concentration

[26] Particulate matters in the atmosphere over Kanpur are loaded by the industrial activities, vehicular emissions,

and resuspended local soil dusts. In addition, dusts transported by the southwesterly winds during the premonsoon season contribute strongly to the  $\text{PM}_{10}$  concentration in this region. The average  $\text{PM}_{10}$  concentrations for the month of May are  $231.6$  and  $167.2 \mu\text{g m}^{-3}$  in 2001 and 2002, respectively, which suggests a very high level of  $\text{PM}_{10}$  concentration in the atmosphere over Kanpur compared to the standards set by CPCB. Daily variations in  $\text{PM}_{10}$  concentration in May 2001 and 2002 are shown in Figures 5c and 5d, respectively. Unfortunately,  $\text{PM}_{10}$  data are missing for some days, which restricted the understanding of the response of the air quality to the dust loading. After each dust event,  $\text{PM}_{10}$  concentration increases by  $\sim 150 \mu\text{g m}^{-3}$  except after the 27 May 2002 event. During the last week of May 2002,  $\text{PM}_{10}$  concentration was been measured to be low ( $< 100 \mu\text{g m}^{-3}$ ). The drop in  $\text{PM}_{10}$  concentration may be due to a sudden change in the transport pattern or scavenging. Relative humidity has been found to increase suddenly from 39% to 67.5% on 24 May 2002 and to remain higher during the next few days. Rainfall has been recorded on 4 May 2001 and on 25, 28,

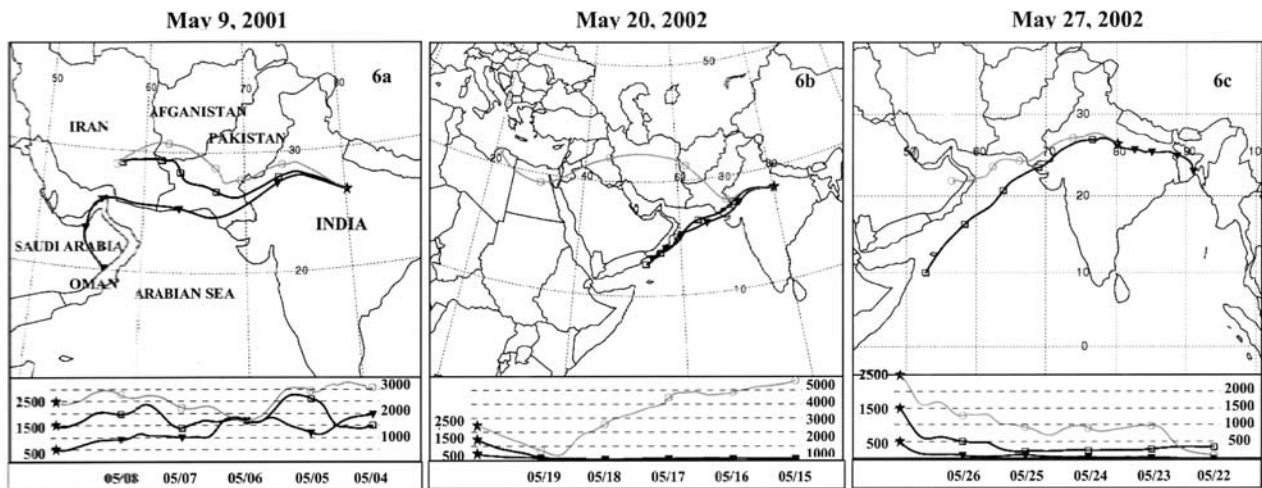


**Figure 6.** The 5-day backward trajectory from (a) 9 May 2001, (b) 20 May 2002, and (c) 27 May 2002 at 500-, 1500-, and 2500-m heights from the surface.

and 29 May 2002 (Figures 5a and 5b) over Kanpur; as a result the  $\text{PM}_{10}$  concentration is found to drop by at least  $100 \mu\text{g m}^{-3}$ . Maximum decrease in  $\text{PM}_{10}$  concentration has been found after 27 May 2002, when the highest rainfall (14.6 mm) has been recorded. Temperature is also observed to drop by  $\sim 5^\circ\text{C}$  from 25 May 2002 onward, which may lead to the decrease in the water-holding capacity of the atmosphere over the region. During the last week of May 2002 the meteorological conditions changed which did not allow the particulate matter to persist in the atmosphere even after the 27 May 2002 event.

[27]  $\text{PM}_{10}$  concentration has also been observed to be very high ( $\sim 400 \mu\text{g m}^{-3}$ ) on 2 May 2001 (Figure 5c). However, no dust event was observed on that day. The value of  $\alpha$  is found to be 0.28 on that day compared to 0.58 one day earlier without much change in AOD. The increase of AOD has been found in the near-infrared wavelengths, whereas AOD decreases in the visible wavelengths, resulting in a change in the overall spectral variation. *Monkkonen et al.* [2004] have found that aerosol number concentration shows an interesting relationship with  $\text{PM}_{10}$  concentration in the polluted urban environment over Delhi in the Indo-Gangetic basin. They have shown that aerosol number concentration initially increases with  $\text{PM}_{10}$  concentration up to  $300 \mu\text{g m}^{-3}$ . Kanpur has a similar environment to that of Delhi; hence the high  $\text{PM}_{10}$  concentration leads to coagulation of the submicron urban aerosols forming coarser particles, resulting in the increase of AOD at the higher wavelengths and decrease in the lower visible wavelengths, i.e., the decrease of the spectral variation. The local sources of particulate matters could not affect the AOD spectra as much as it has been affected by the dust events.

#### 4.7. Source and Transport of the Dusts

[28] With a view to study the role of transport in carrying the dust particles over the Indo-Gangetic basin during the dust events, 3-day trajectories have been computed using the Hybrid Single-Particle Lagrangian Integrated Trajectory (HY-SPLIT) model of the National Oceanic and Atmospheric Administration (NOAA), United States (available at <http://www.arl.noaa.gov/ready/hysplit4.html>). Figures 6a–6c

show 5-day backward trajectories from 9 May 2001 and 20 and 27 May 2002 to locate the path of the dust-carrying air mass to the region at altitudes of 500 m, the mixed layer; 1500 m, above the boundary layer where the dusts are lifted by convection and transported over long distance; and 2500 m, the relatively free troposphere.

[29] The wind in the mixed layer is responsible for raising the loose soil dust particles in the atmosphere. In all the three trajectories, air mass has been close to the surface while passing over the western Thar Desert before reaching the Indo-Gangetic basin. Also, it is evident that the air mass at 2500-m altitude is coming from the gulf regions in all cases. Only for the 20 May 2002 event, was the higher-altitude air mass close to the surface while passing over the gulf regions, thus adding as another source to the transported dusts, whereas in all other dust events, only the Thar Desert is likely to be the main source. It is clear from the back trajectory of 27 May 2002 that the dusts are advected above the boundary layer, which is another reason for not affecting the  $\text{PM}_{10}$  concentration at the ground level. The back trajectory model shows the air mass also originating from the eastern part of the Indo-Gangetic basin on that day, altering the optical properties of the aerosols during the event observed on 27 May 2002.

[30] Figure 7 shows variation of TOMS AI during all the dust events over the Indo-Gangetic basin, which shows regional distribution of aerosols. The AI ranging from 1.7 to 3.2 in the images marks the spreading of the dusts in the atmosphere. The dusts were seen over the Thar region on 7 May 2001 and then spread over the Indo-Gangetic basin on 8 and 9 May. Similar observations have also been made on 19 and 20 May 2002. Higher AI values have been observed over Kanpur in the most intense dust storm event of 20 May 2002 showing a pronounced effect on the optical properties of the aerosols. In the eastern part of the basin, an AI of more than 3.7 has been found on 19 May 2002, which is attributed to the presence of the absorbing aerosols. After the two dust storms on 19 and 20 May the dusts were transported toward the eastern part of the Indo-Gangetic basin. Both from the trajectory and AI images, it is clear that the dust originated from the Thar Desert, whereas the gulf

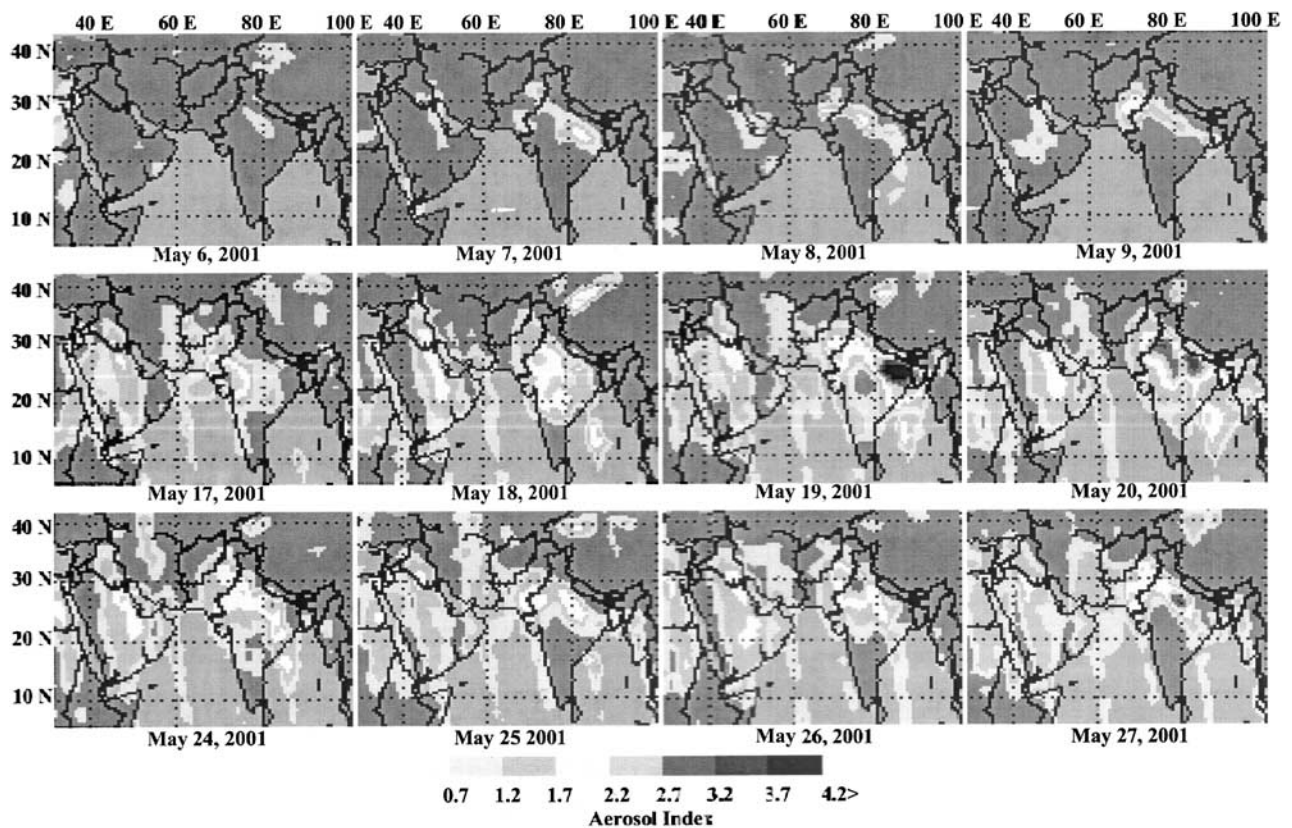


**Figure 7.** Total Ozone Mapping Spectrometer (TOMS) aerosol index images showing the source and the progressive movement of the dusts over the Indo-Gangetic basin during the dust storms.

regions only contribute to the 20 May 2002 event. The AI image on 27 May 2002 (Figure 7) confirms the presence of the dusts along with absorbing aerosols ( $AI > 3.7$  is seen over Kanpur). The backward trajectory on 27 May (Figure 6c) shows that the wind in the mixed layer, very close to the surface from 22 May onward, was flowing from the east toward Kanpur.

[31] The regional distribution of aerosols interpreted from AI images corresponds well with the changes in the optical properties observed in Kanpur. The transport paths are also favorable to bring the aerosols in and out of Kanpur. The optical properties have been found to change in response to the changing nature of the aerosol loading over the Indo-Gangetic basin. Unfortunately, because of the nonavailability of chemical data it is difficult to comment on the source of the dusts in terms of mineralogy; but the back trajectories and AI images clearly indicate the transport of dusts from the western Thar Desert over this region during the dust storms.

## 5. Conclusions

[32] The dust events are found to affect the optical properties of the aerosols over the Indo-Gangetic basin significantly. The major conclusions drawn from the present study are the following:

[33] 1. The Indo-Gangetic basin is characterized by high AOD during the premonsoon season. The AOD spectrum is mainly controlled by the local diurnal variation in aerosol

loading, but the dusts transported from the western Thar Desert by southwesterly winds have a strong impact on the AOD spectrum. AOD has been found to increase to even higher values (sometimes AOD rises above 1), but the rise is greater at the higher wavelengths compared to the lower wavelengths, reducing the spectral variation. This is reflected in very low values ( $<0.2$ ) of the angstrom parameter.

[34] 2.  $PM_{10}$  concentration in the Indo-Gangetic basin is strongly controlled by the local pollutant cycle but has been found to increase drastically after all the dust events, except on 27 May 2002, when the particulate matters are scavenged out of the atmosphere because of precipitation and the dust layer is advected to a higher level; as a result, no change in ground level  $PM_{10}$  concentration is observed.

[35] 3. Significant impacts of dust events in changing the optical properties of the aerosols at higher wavelengths ( $\lambda > 440$  nm) are found over the Indo-Gangetic basin. The 27 May 2002 event makes the optical state of the atmosphere absorbing, whereas the other events make it scattering. This contrasting nature of the optical state of the atmosphere during dust loading is due the influx of biomass burning (absorbing) aerosols from the eastern part of the basin on 27 May 2002. In general, the region is characterized by an abundance of urban aerosol of which sulfate is the dominant one, which is scattering in nature. In addition to that, dust storms induce more scattering particles into the atmosphere, making the optical state scattering. The variations of the refractive indices, both real and imaginary,

during the study period support the characterization of the aerosol loading, interpreted from SSA values.

[36] 4. Size distribution of the aerosols over the Indo-Gangetic basin is found to be bimodal, but because of the particle growth in high relative humidity a third mode is appearing around 1  $\mu\text{m}$  size range during the premonsoon and monsoon seasons. The dust storms induce a huge increase in the volume concentration at the coarse mode but have no effect on the volume concentration at the fine mode. The 27 May 2002 event results in modifying the size distribution at both fine and coarse mode.

[37] 5. Successive TOMS AI images have been used to support the characterization of the aerosols in terms of their optical properties. Both the air mass trajectories and TOMS AI images have shown that the Thar Desert is the main source of the dusts, whereas the Gulf region only contributes to the 20 May 2002 event.

[38] **Acknowledgments.** The work is supported through research projects (DST-ICRP and ISRO-GBP). The CIMEL is operational on IIT Kanpur campus through NASA – IIITK agreement. The PM<sub>10</sub> concentration data are available through Central Pollution Control Board (<http://cpbc.nic.in>) and the aerosol index data has been downloaded from TOMS web site (<http://toms.gsfc.nasa.gov>). The ray trajectories are computed from the FNL data archive in NOAA Air Resources Laboratory using HYSPLIT models. We are also grateful to two anonymous reviewers for their constructive comments.

## References

- Angstrom, A. (1964), The parameters of atmospheric turbidity, *Tellus*, *16*, 64–75.
- Bohren, C. F., and D. R. Huffman (1983), *Absorption and Scattering of Light by Small Particles*, 550 pp., John Wiley, Hoboken, N. J.
- Bonasoni, P., P. Cristofanelli, F. Calzolari, U. Bonafe, F. Evangelisti, A. Stohl, R. van Dingenen, T. Colombo, and Y. Balkanski (2004), Aerosol-ozone correlations during dust transport episodes, *Atmos. Chem. Phys.*, *4*, 2055–2088.
- Dickerson, R. R., S. Kondragunta, G. Stenchikov, K. L. Civerolo, B. G. Doddridge, and B. N. Holben (1997), The impact of aerosols on solar ultraviolet radiation and photochemical smog, *Science*, *278*, 827–830.
- Dubovik, O., and M. D. King (2000), A flexible inversion algorithm for retrieval of aerosol optical properties from Sun and sky radiance measurements, *J. Geophys. Res.*, *105*, 20,673–20,696.
- Dubovik, O., A. Smirnov, B. N. Holben, M. D. King, Y. J. Kaufman, T. F. Eck, and I. Slutsker (2000), Accuracy assessments of aerosol optical properties retrieved from Aerosol Robotic Network (AERONET) Sun and sky radiance measurements, *J. Geophys. Res.*, *105*, 9791–9806.
- Dubovik, O., B. N. Holben, T. F. Eck, A. Smirnov, Y. J. Kaufman, M. D. King, D. Tanre, and I. Slutsker (2002a), Variability of absorption and optical properties of key aerosol types observed in worldwide locations, *J. Atmos. Sci.*, *59*, 590–608.
- Dubovik, O., B. N. Holben, T. Lapyonok, A. Sinyuk, M. I. Mishchenko, P. Yang, and I. Slutsker (2002b), Non-spherical aerosol retrieval method employing light scattering by spheroids, *Geophys. Res. Lett.*, *29*(10), 1415, doi:10.1029/2001GL014506.
- Eck, T. F., B. N. Holben, J. S. Reid, O. Dubovik, A. Smirnov, N. T. O'Neill, I. Slutsker, and S. Kinne (1999), Wavelength dependence of the optical depth of biomass burning, urban, and desert dust aerosols, *J. Geophys. Res.*, *104*, 31,333–31,349.
- Guttikunda, S. K., G. R. Carmichael, G. Calori, C. Eck, and J.-H. Woo (2003), The contribution of megacities to regional sulfur pollution in Asia, *Atmos. Environ.*, *37*, 11–22.
- Hamonou, E., P. Chazette, D. Balis, F. Dulac, X. Schneider, E. Galani, E. Ancellet, and A. Papayannis (1999), Characterization of the vertical structure of Saharan dust export to the Mediterranean basin, *J. Geophys. Res.*, *104*, 22,257–22,270.
- Hansen, J. E., and L. D. Travis (1974), Light scattering in planetary atmosphere, *Space Sci. Rev.*, *16*, 527–610.
- Hansen, J., M. Sato, and R. Ruedy (1997), Radiative forcing and climate response, *J. Geophys. Res.*, *102*, 6831–6864.
- Hartley, W. S., P. V. Hobbs, J. L. Ross, P. B. Russell, and J. M. Livingston (2000), Properties of aerosols aloft relevant to direct radiative forcing of the mid-Atlantic coast of the United States, *J. Geophys. Res.*, *105*, 9859–9885.
- Hegg, D. A., J. Livingston, P. V. Hobbs, T. Novakov, and P. Russell (1997), Chemical apportionment of aerosol column optical depth off the mid-Atlantic coast of the United States, *J. Geophys. Res.*, *102*, 25,293–25,303.
- Herman, J. R., P. K. Bhartia, O. Torres, C. Hsu, C. Seftor, and E. Celarier (1997), Global distribution of UV-absorbing aerosols from Nimbus 7/TOMS data, *J. Geophys. Res.*, *102*, 16,911–19,922.
- Hess, M., P. Koepke, and I. Schult (1998), Optical properties of aerosols and clouds: The software package OPAC, *Bull. Am. Meteorol. Soc.*, *79*(5), 831–844.
- Holben, B., et al. (1998), AERONET—A federated instrument network and data archive for aerosol characterization, *Remote Sens. Environ.*, *66*(1), 1–16.
- Hoppel, W. A., J. W. Fitzgerald, and R. E. Larson (1985), Aerosol size distributions in air masses advecting off the east coast of the United States, *J. Geophys. Res.*, *90*, 2365–2379.
- Husar, R. B., J. M. Prospero, and L. L. Stowe (1997), Characterization of tropospheric aerosols over the oceans with the NOAA advanced very high resolution radiometer optical thickness operational product, *J. Geophys. Res.*, *102*, 16,889–16,909.
- Husar, R. B., et al. (2001), Asian dust events of April 1998, *J. Geophys. Res.*, *106*, 18,317–18,330.
- Joseph, P. V. (1982), A tentative model of Andhi, *Mausam*, *3*, 417–420.
- Koepke, P., M. Hess, I. Schult, and E. P. Shettle (1997), Global aerosol data set, *Rep.*, *243*, 44 pp., Max Planck Inst. for Meteorol., Hamburg, Germany.
- Kotchenruther, R., P. V. Hobbs, and D. A. Hegg (1999), Humidification factors for atmospheric aerosols off the mid-Atlantic coast of the United States, *J. Geophys. Res.*, *104*, 2239–2251.
- Léon, J.-F., and M. Legrand (2003), Mineral dust sources in the surroundings of the north Indian Ocean, *Geophys. Res. Lett.*, *30*(6), 1309, doi:10.1029/2002GL016690.
- Levin, Z., J. H. Joseph, and Y. Mekler (1980), Properties of Sharav (Khamsin) dust—Comparison of optical and direct sampling data, *J. Atmos. Sci.*, *37*, 182–191.
- Middleton, N. J. (1986a), Dust storms in the middle east, *J. Arid Environ.*, *10*, 83–96.
- Middleton, N. J. (1986b), A geography of dust storms in southwest Asia, *J. Clim.*, *6*, 183–196.
- Mishchenko, M. I., and L. D. Travis (1994), T-matrix computations of light scattering by large spheroidal particles, *Opt. Commun.*, *109*, 16–21.
- Mishchenko, M. I., A. A. Lacis, B. E. Carlson, and L. D. Travis (1995), Nonsphericity of dust-like tropospheric aerosols: Implications for aerosol remote sensing and climate modeling, *Geophys. Res. Lett.*, *22*(9), 1077–1080.
- Mishchenko, M. I., L. D. Travis, R. A. Kahn, and R. A. West (1997), Modeling phase functions for dust-like tropospheric aerosols using a shape mixture of randomly oriented polydisperse spheroids, *J. Geophys. Res.*, *102*, 16,831–16,847.
- Mishchenko, M. I., J. W. Hovenir, and L. D. Travis (2000), *Light Scattering by Nonspherical Particles*, 690 pp., Academic, San Diego, Calif.
- Mitra, A. P., and C. Sharma (2002), Indian aerosols: Present status, *Chemosphere*, *49*, 1175–1190.
- Monkkonen, P., R. Uma, D. Srinivasan, I. K. Koponen, K. E. J. Lehtinen, K. Hameri, R. Suresh, V. P. Sharma, and M. Kulmala (2004), Relationship and variations of aerosol number and PM<sub>10</sub> mass concentrations in a highly polluted urban environment—New Delhi, India, *Atmos. Environ.*, *38*, 425–433.
- Negi, B. S., S. Sadasivan, K. S. V. Nambi, and B. M. Pandey (1996), Characterization of atmospheric dust at Gurushikar, Mt. Abu, Rajasthan, *Environ. Monit. Assess.*, *40*(3), 253–259.
- O'Neill, N. T., T. F. Eck, B. N. Holben, A. Smirnov, O. Dubovik, and A. Royer (2001), Bi-modal size distribution influences on the variation of Angstrom derivatives in spectral and optical depth space, *J. Geophys. Res.*, *106*, 9787–9806.
- Otterman, J., R. S. Fraser, and O. P. Bahethi (1982), Characterization of tropospheric desert aerosols at solar wavelengths by multispectral radiometry from Landsat, *J. Geophys. Res.*, *87*, 1270–1278.
- Parameswaran, K., and G. Vijayakumar (1994), Effect of relative humidity on aerosol size distribution, *Indian J. Radio Space Phys.*, *23*(3), 175–188.
- Pease, P. P., V. P. Tchakerian, and N. W. Tindale (1998), Aerosols over the Arabian Sea: Geochemistry and source areas for aeolian desert dust, *J. Arid Environ.*, *39*, 477–496.
- Prospero, J. M. (1999), Long-term measurements of the transport of African mineral dust to the southeastern United States: Implications for regional air quality, *J. Geophys. Res.*, *104*, 15,917–15,927.
- Prospero, J. M., R. Schmitt, E. Cuevas, D. L. Savoie, W. C. Graustein, K. K. Turekian, A. Volz-Thomas, A. Diaz, S. J. Oltmans, and H. Levi II (1995), Temporal variability of summer time ozone and aerosol in the

- free troposphere over the eastern North Atlantic, *Geophys. Res. Lett.*, **22**(21), 2925–2928.
- Prospero, J. M., P. Ginoux, O. Torres, S. E. Nicholson, and T. E. Gill (2002), Environmental characterization of global sources of atmospheric soil dust identified with the Nimbus 7 Total ozone Mapping Spectrometer (TOMS) absorbing aerosol product, *Rev. Geophys.*, **40**(1), 1002, doi:10.1029/2000RG000095.
- Reddy, M. S., and C. Venkataraman (2002), Inventory of aerosol and sulfur di-oxide emissions from India: part II-Biomass combustion, *Atmos. Environ.*, **36**, 699–712.
- Russell, P. B., J. Livingston, P. Hignett, S. Kinne, J. Wong, A. Chien, R. Bergstrom, P. Durkee, and P. Hobbs (1999), Aerosol-induced radiative flux changes off the United States mid-Atlantic coast: Comparison of values calculated from sunphotometer and in situ data with those measured by airborne pyranometer, *J. Geophys. Res.*, **104**, 2289–2307.
- Satheesh, S. K., V. Ramanathan, X. Li-Jones, J. M. Lobert, I. A. Podgorny, J. M. Prospero, B. N. Holben, and N. G. Loeb (1999), A model for natural and anthropogenic aerosols over the tropical Indian Ocean derived from Indian Ocean Experiment data, *J. Geophys. Res.*, **104**, 27,421–27,440.
- Sharma, M., Y. N. V. M. Kiran, and K. K. Shandilya (2003), Investigations into formation of atmospheric sulfate under high PM<sub>10</sub> concentration, *Atmos. Environ.*, **37**, 2005–2013.
- Shettle, E. P., and R. W. Fenn (1979), Models of aerosols lower troposphere and the effect of humidity variations on their optical properties, *AFCRL Tech. Rep. 79 0214*, 100 pp., Air Force Cambridge Res. Lab., Hanscom Air Force Base, Mass.
- Sikka, D. R. (1997), Desert climate and its dynamics, *Curr. Sci.*, **72**(1), 35–46.
- Smirnov, A., B. N. Holben, I. Slutsker, E. J. Welton, and P. Formenti (1998), Optical properties of Saharan dust during ACE-2, *J. Geophys. Res.*, **103**, 28,079–28,092.
- Smirnov, A., B. N. Holben, T. F. Eck, O. Dubovik, and I. Slutsker (2000), Cloud screening and quality control algorithms for the AERONET database, *Remote Sens. Environ.*, **73**(3), 337–349.
- Smirnov, A., B. N. Holben, T. F. Eck, I. Slutsker, B. Chatanet, and R. T. Pinker (2002), Diurnal variability of aerosol optical depth observed at AERONET (Aerosol Robotic Network) sites, *Geophys. Res. Lett.*, **29**(23), 2115, doi:10.1029/2002GL016305.
- Sokolik, I. N., and O. B. Toon (1999), Incorporation of mineralogical composition into models of the radiative properties of mineral aerosol from UV to IR wavelengths, *J. Geophys. Res.*, **104**, 9423–9444.
- Sokolik, I. N., A. Andronove, and T. C. Johnson (1993), Complex refractive index of atmospheric dust aerosols, *Atmos. Environ., Part A*, **27**, 2495–2502.
- Tanre, D., Y. J. Kaufman, B. N. Holben, B. Chatanet, A. Karnieli, F. Lavenu, L. Blarel, O. Dubovik, L. A. Remer, and A. Smirnov (2001), Climatology of dust aerosol size distribution and optical properties derived from remotely sensed data in the solar spectrum, *J. Geophys. Res.*, **106**, 18,205–18,217.
- Tanre, D., J. Haywood, J. Pelon, J. F. Leon, B. Chatanet, P. Formenti, P. Francis, P. Goloub, E. J. Highwood, and G. Myhre (2003), Measurement and modeling of the Saharan dust radiative impact: Overview of the Saharan Dust Experiment (SHADE), *J. Geophys. Res.*, **108**, 8574, doi:10.1029/2002JD003273.
- Tegen, I. A., and A. A. Lacis (1996), Modeling of particle size distribution and its influence on the radiative properties of mineral dust aerosols, *J. Geophys. Res.*, **101**, 19,237–19,244.
- Tegen, I., A. A. Lacis, and I. Fung (1996), The influence on climate forcing of mineral aerosols from disturbed soils, *Nature*, **380**, 419–422.
- Torres, O., P. K. Bhartia, J. R. Herman, Z. Ahmad, and J. Gleason (1998), Derivation of aerosol properties from satellite measurements of backscattered ultraviolet radiation: Theoretical basis, *J. Geophys. Res.*, **103**, 17,099–17,110.
- Tripathi, J. K., and V. Rajamani (1999), Geochemistry of the loessic sediments on Delhi ridge, eastern Thar Desert, Rajasthan: Implications for exogenic processes, *Chem. Geol.*, **155**, 265–278.
- Washington, R., M. Todd, N. J. Middleton, and A. S. Goudie (2003), Dust storm source areas determined by the Total Ozone Monitoring Spectrometer and surface observations, *Ann. Assoc. Am. Geogr.*, **93**, 297–313.
- World Meteorological Organization (WMO) (1983), Radiation commission of IAMAP meeting of experts on aerosols and their climatic effects, *Rep. WCP55*, Geneva, Switzerland.
- Yadav, S., and V. Rajamani (2003), Aerosols of NW India—A potential Cu source!, *Curr. Sci.*, **84**(3), 278–280.

S. Dey and S. N. Tripathi, Department of Civil Engineering, Indian Institute of Technology, Kanpur–208 016, India. (sagnik@iitk.ac.in; snt@iitk.ac.in)

B. N. Holben, NASA Goddard Space Flight Center, Greenbelt, MD 20771, USA. (brent@aeronet.gsfc.nasa.gov)

R. P. Singh (corresponding author), School of Computational Sciences, George Mason University, Fairfax, VA 22030, USA. (rsingh3@gmu.edu)